Influence of short-range spin correlations on the μSR polarization functions in the slow dynamic limit: Application to the quantum spin-liquid system $Yb_2Ti_2O_7$

A. Yaouanc
Laboratory for Muon-Spin Spectroscopy, Paul Scherrer Institute, CH-5232 Villigen-PSI, Switzerland and Institut Nanosciences et Cryogénie, SPSMS, CEA and Université Joseph Fourier, F-38054 Grenoble, France

A. Maisuradze
Physik-Institut der Universität Zürich, Winterthuerstrasse 190, CH-8057 Zürich, Switzerland and Laboratory for Muon-Spin Spectroscopy, Paul Scherrer Institute, CH-5232 Villigen-PSI, Switzerland

P. Dalmas de Réotier
Institut Nanosciences et Cryogénie, SPSMS, CEA and Université Joseph Fourier, F-38054 Grenoble, France
(Received 25 January 2013; revised manuscript received 21 March 2013; published 5 April 2013)

Here we discuss how to account for short-range spin correlations on the measured muon spin relaxation spectra. The shape of the zero-field relaxation function is found to be highly sensitive to short-range spin correlations, as clearly inferred from the analysis of the published longitudinal relaxation function for the pyrochlore quantum spin-liquid system $Yb_2Ti_2O_7$ at low temperature. The field distribution at the muon site in this compound is found to be strongly asymmetric, i.e., to deviate substantially from the usually expected Gaussian function. This is a clear signature of short-range correlations of the spins. Our analysis yields the characteristic function of the component field distribution at the muon site of $Yb_2Ti_2O_7$, a well-defined statistical physics quantity accessible to theory once an interaction Hamiltonian is available and the muon site is determined. As a by-product of our study, we have found that the validity of the so-called golden formula due to Kubo is limited.

DOI: 10.1103/PhysRevB.87.134405 PACS number(s): 75.10.Jm, 05.40.−a, 76.75.+i

A slow spin dynamic has been detected for spin glasses, a few highly disordered magnetic systems, and some geometrically frustrated magnetic materials using the ac susceptibility, positive muon spin relaxation (μSR), and neutron spin echo (NSE) techniques; see for example Refs. 1–7. Key information of interest is the nature of the short-range spin correlations. Although of much interest, their microscopic characterization is difficult because the number of experimental techniques available for probing these correlations is restricted. The muon being a local probe is sometimes believed not to be able to provide information on the extension of these correlations. However, an experimentally observed shallow μSR polarization function minimum has been interpreted as a signature of short-range spin correlations using results of Monte Carlo simulations.[8] Originally the μSR spectra were analyzed with a phenomenological extension of the usual Kubo-Toyabe model with no obvious connection with the numerically inferred short-range correlations.[2] Based on well-established statistical methods, here we show how to describe analytically the effect of short-range spin correlations. Our work should help to extract microscopic information on these correlations. As an example of application, from the published longitudinal-field polarization function measured for the quantum spin-liquid system $Yb_2Ti_2O_7$ we extract the component field distribution at the muon site and the related characteristic function for this compound.

The μSR technique best suited to study the magnetic correlations is the so-called longitudinal one for which the initial muon beam polarization and the external field $\mathbf{B}_{\rm ext}$, if any, are parallel.[9–11] By definition, they are both parallel to the Z direction. We complete the laboratory orthogonal reference frame with the X and Y axes. Results are also obtained with the transverse geometry for which $\mathbf{B}_{\rm ext}$ is still parallel to the Z axis, but the initial polarization is taken to be along the X axis. A longitudinal measurement gives access to the longitudinal polarization function, $P_Z(t)$ with $P_Z(t=0)=1$. In the transverse geometry, it is the $P_X(t)$ function which is measured. Two limiting cases have to be distinguished. In the first case the spin dynamics is fast and the motional narrowing limit applies. For a single crystal $P_Z(t)$ is then an exponential function[12] and therefore is characterized by a spin-lattice relaxation rate λ_Z. We are in fact using the nuclear magnetic resonance language.[13,14] In the same fast fluctuation limit and if $B_{\rm ext}$ is sufficiently intense, the envelope of $P_X(t)$ is an exponential function, the decay of which is given by the spin-spin relaxation rate λ_X. For both experimental geometries, conventional methods based on the use of the frequency and wave vector dependent susceptibility can then be applied to describe the effect of the spin correlations.[10,15,16] In the other limit, i.e., in the slow dynamic limit, the dynamics may become so slow that the magnetic field distribution at the muon sites which drives the muon spin ensemble is of quasistatic nature. It is this physical case which is of interest here.

The method used in this work for the description of short-range correlations is based on well-known concepts of statistical physics. Usual practice assumes a Gaussian field component distribution. Implicitly it means that the short-range correlations are neglected. To account for them here the distribution is generalized as expressed by Eqs. (19), (20), (21); see below. This approach should be used if the physics of the system under study is not well known. On the other hand, if its Hamiltonian is known it may be more appropriate to start from the characteristic function of the distribution. Its definition is given in Eq. (4). To get the text accessible the

definitions of the two polarization functions are given and a number of plots are presented. They should be useful when considering the analysis of experimental data.

In a first step we shall assume the field distribution at the muon site to be static. The slow dynamic will be introduced later on. Focusing mainly on the longitudinal geometry, we shall start by describing the static polarization function, $P_Z^{\rm stat}(t)$. With the additional temporary assumption $\mathbf{B}_{\rm ext}=0$, the local field at a muon site $\mathbf{B}_{\rm loc}$ only arises from the interaction of the muon spins with the magnetic moments of the compound under study. The relation between $\mathbf{B}_{\rm loc}$ and the magnetic moments is linear and is described by a tensor. The magnetic moments induce a vector field distribution at the muon sites, $D_{\rm v}(\mathbf{B}_{\rm loc})$. With these assumptions,[16]

$$P_Z^{\rm stat}(t)=\int\left\{\left(\frac{B_{\rm loc}^Z}{B_{\rm loc}}\right)^2+\left[1-\left(\frac{B_{\rm loc}^Z}{B_{\rm loc}}\right)^2\right]\cos(\omega_\mu t)\right\}\times D_{\rm v}(\mathbf{B}_{\rm loc})d^3\mathbf{B}_{\rm loc}. \tag{1}$$

The integral extends over all the possible $\mathbf{B}_{\rm loc}$ values and $\omega_\mu=\gamma_\mu[(B_{\rm loc}^X)^2+(B_{\rm loc}^Y)^2+(B_{\rm loc}^Z)^2]^{1/2}$, where $\gamma_\mu=851.615$ Mrad $\rm s^{-1}$ $\rm T^{-1}$ is the muon gyromagnetic ratio. Since our purpose is to unravel correlation effects, without any concern of the possible $\mathbf{B}_{\rm loc}$ anisotropy, for simplicity $D_{\rm v}(\mathbf{B}_{\rm loc})$ is taken as the product of the three Cartesian component distributions:

$$D_{\rm v}(\mathbf{B}_{\rm loc})d^3\mathbf{B}_{\rm loc}=D_{\rm c}\big(B_{\rm loc}^X\big)D_{\rm c}\big(B_{\rm loc}^Y\big)D_{\rm c}\big(B_{\rm loc}^Z\big)dB_{\rm loc}^X dB_{\rm loc}^Y dB_{\rm loc}^Z, \tag{2}$$

where $D_{\rm c}(B_{\rm loc}^\alpha)$ is the component field distribution along the α direction. From this discussion, we derive

$$P_Z^{\rm stat}(t)=\frac{1}{3}+\frac{2}{3}\iiint_{-\infty}^{\infty}D_{\rm c}\big(B_{\rm loc}^X\big)D_{\rm c}\big(B_{\rm loc}^Y\big)D_{\rm c}\big(B_{\rm loc}^Z\big)\times\cos(\omega_\mu t)dB_{\rm loc}^X dB_{\rm loc}^Y dB_{\rm loc}^Z. \tag{3}$$

Here, for simplicity we assume identical component field distributions $D_{\rm c}(B_{\rm loc}^\alpha)$ ($\alpha=X$, Y, or Z). We shall stay with the Cartesian coordinates for this whole work.

The distributions of a many-body system, such as interacting magnetic moments, are often of Gaussian nature. Since the relation between the moments and $\mathbf{B}_{\rm loc}$ is linear, $D_{\rm c}(B_{\rm loc}^\alpha)$ is also bound to be Gaussian. This leads to the famous Kubo-Toyabe $P_Z^{\rm stat}(t)$ function for which the mean field value is obviously zero; i.e., the spontaneous field vanishes.

However, for highly correlated systems deviations from the Gaussian have been observed. In order to account for them we consider the characteristic function $G(t)$:[17–19]

$$G(t)=\int_{-\infty}^{\infty}\exp\big(i\gamma_\mu B_{\rm loc}^\alpha t\big)D_{\rm c}\big(B_{\rm loc}^\alpha\big)dB_{\rm loc}^\alpha. \tag{4}$$

Here, for simplicity and without risk of confusion, we write $G(t)$ rather than $G^\alpha(t)$. This is justified since the $D_c(B_{\rm loc}^\alpha)$ functions are taken identical for all α. An elegant solution for the longitudinal polarization function defined by Eq. (3) was proposed by Kubo:[20,21]

$$P_Z^{\rm stat}(t)=\tfrac{1}{3}+\tfrac{2}{3}[Q(t)+tQ'(t)], \tag{5}$$

where[16]

$$Q(t)=\mathrm{Re}\{G(t)\}. \tag{6}$$

The real part of $G(t)$ is denoted by $\mathrm{Re}\{G(t)\}$. From the Fourier theorem,

$$D_{\rm c}\big(B_{\rm loc}^\alpha\big)=\gamma_\mu\int_{-\infty}^{\infty}\exp\big(-i\gamma_\mu B_{\rm loc}^\alpha t\big)G(t)\frac{dt}{2\pi}. \tag{7}$$

Referring to its definition given in Eq. (4), $G(t)$ can be expanded in a Maclaurin series whose coefficients are the moments of the component distribution:

$$G(t)=\sum_{n=0}^{\infty}\frac{(i\gamma_\mu t)^n}{n!}\big\langle\big(B_{\rm loc}^\alpha\big)^n\big\rangle, \tag{8}$$

with the nth moment

$$\big\langle\big(B_{\rm loc}^\alpha\big)^n\big\rangle=\int_{-\infty}^{\infty}\big(B_{\rm loc}^\alpha\big)^n D_{\rm c}\big(B_{\rm loc}^\alpha\big)dB_{\rm loc}^\alpha. \tag{9}$$

However, it is more useful to consider the logarithm of $G(t)$ as an expansion in cumulants:

$$\ln G(t)=\sum_{n=1}^{\infty}\frac{(i\gamma_\mu t)^n}{n!}\kappa_n, \tag{10}$$

where κ_n is the nth cumulant. In terms of the moments, for the first four cumulants we have the relations

$$\kappa_1=\big\langle B_{\rm loc}^\alpha\big\rangle,\quad \kappa_2=\Delta^2,\quad \kappa_3=\big\langle\big(B_{\rm loc}^\alpha-\big\langle B_{\rm loc}^\alpha\big\rangle\big)^3\big\rangle,\quad \kappa_4=\big\langle\big(B_{\rm loc}^\alpha-\big\langle B_{\rm loc}^\alpha\big\rangle\big)^4\big\rangle-3\Delta^4, \tag{11}$$

where $\langle B_{\rm loc}^\alpha\rangle$ is the mean field at the muon site, i.e., the first moment of $D_{\rm c}(B_{\rm loc}^\alpha)$, and Δ is its standard deviation. In fact, for κ_3 and κ_4 we have introduced central moments which are moments about $\langle B_{\rm loc}^\alpha\rangle$.[17] Normalizing the cumulant expansion with Δ,

$$\ln G(t)=i\gamma_\mu\big\langle B_{\rm loc}^\alpha\big\rangle t+\sum_{n=2}^{\infty}\frac{(i\gamma_\mu\Delta\nu_n t)^n}{n!}. \tag{12}$$

Here $\nu_2=1$ and the parameters ν_n with $n\geqslant 3$ characterize the deviation of $D_{\rm c}(B_{\rm loc}^\alpha)$ from the Gaussian form. For instance, ν_3 is the skewness and ν_4 the kurtosis. They are related to cumulants.[17] Specifically,

$$\nu_3=\kappa_3/\kappa_2^{3/2},\quad \nu_4=\kappa_4/\kappa_2^2, \tag{13}$$

and in general,

$$\nu_n=\kappa_n/\kappa_2^{n/2}. \tag{14}$$

Rather than the kurtosis, the so-called excess kurtosis is sometimes used. It is defined by $\tilde{\nu}_4=\tilde{\kappa}_4/\kappa_2^2$ with $\tilde{\kappa}_4=\langle(B_{\rm loc}^\alpha-\langle B_{\rm loc}^\alpha\rangle)^4\rangle$. Combining Eqs. (7) and (12) and setting $x=\gamma_\mu t\Delta$,

$$D_{\rm c}\big(B_{\rm loc}^\alpha\big)=\frac{1}{\Delta}\int_{-\infty}^{\infty}\exp\left[i\frac{\langle B_{\rm loc}^\alpha\rangle-B_{\rm loc}^\alpha}{\Delta}x+\sum_{n=2}^{\infty}\frac{(i\nu_n x)^n}{n!}\right]\frac{dx}{2\pi}. \tag{15}$$

Therefore, instead of $D_c(B^\alpha_{loc})$, we need to consider $\Delta \times D_c(B^\alpha_{loc})$. This distribution is a function of $(\langle B^\alpha_{loc}\rangle - B^\alpha_{loc})/\Delta$, and the parameters ν_n, $\nu_n \geqslant 3$ ($\nu_2 = 1$), which account for the deviation from the Gaussian. When all the ν_n with n odd vanish, $D_c(B^\alpha_{loc})$ is symmetric and independent of ν_n signs. Terms with n odd introduce asymmetry in $D_c(B^\alpha_{loc})$ and therefore induce a finite contribution to $\langle B^\alpha_{loc}\rangle$. In addition, the polarization function is independent of the ν_n signs with n odd, provided the signs of all the ν_n parameters as well as $\langle B^\alpha_{loc}\rangle$ are changed simultaneously.

When the ν_n parameters can be evaluated, i.e., when the cumulant expansion of the logarithm of the characteristic function can be written, according to Eq. (15) $\Delta \times D_c(B^\alpha_{loc})$ can be derived by Fourier transform. Then it is a simple matter to obtain numerically $P^{stat}_Z(t)$ from Eq. (3).

Let us assume that no spontaneous field is observed at the temperature of interest. Then we can study $P^{stat}_X(t)$ with the transverse geometry. For large enough B_{ext}, $P^{stat}_X(t)$ can be expressed as follows:[16]

$$P^{stat}_X(t) = \mathrm{Re}\{G(t)\}\cos(\gamma_\mu B_{ext} t) - \mathrm{Im}\{G(t)\}\sin(\gamma_\mu B_{ext} t), \tag{16}$$

where $\mathrm{Im}\{G(t)\}$ is the imaginary part of $G(t)$. Obviously, if $\Delta \times D_c(B^\alpha_{loc})$ is even $G(t)$ is real, and it is the envelope of $P^{stat}_X(t)$. For simplicity we have neglected any frequency shift.

As an example of the computation of $\Delta \times D_c(B^\alpha_{loc})$ using the characteristic function, we cite the case of the low-temperature phase of the classical XY model in two dimensions. In fact, to compute $G(t)$ at the muon site we need to describe the linear coupling between the muon spin and the magnetic moments of the compound. For simplicity we assume the local field at the muon site to be proportional to the magnetic order parameter. In addition, we take the constant of proportionality to be equal to 1. According to Bramwell *et al*. the probability density function of the fluctuating magnetic order parameter of the XY magnetic system is described by the following characteristic function:[22]

$$\ln G(t) = i\gamma_\mu \langle B^\alpha_{loc}\rangle t - \sum_{\mathbf{q}\neq 0} h(\mathbf{q}), \tag{17}$$

with

$$h(\mathbf{q}) = \frac{i}{2}\sqrt{\frac{2}{g_2}}\frac{G(\mathbf{q})}{N}\gamma_\mu t\Delta - \frac{i}{2}\arctan\left(\sqrt{\frac{2}{g_2}}\frac{G(\mathbf{q})}{N}\gamma_\mu t\Delta\right) + \frac{1}{4}\ln\left[1 + (\gamma_\mu t\Delta)^2\frac{2}{g_2}\frac{G^2(\mathbf{q})}{N^2}\right]. \tag{18}$$

Here, we have introduced the Green's function in Fourier space $G(\mathbf{q}) = (4 - 2\cos q_x - 2\cos q_y)^{-1}$ with two-dimensional $\mathbf{q}$ vector: $q_x = (2\pi/L)m$ and $q_y = (2\pi/L)n$. The parameter L determines the size of the 2-dimensional magnetic cluster $N = L^2$ (in the present case $L = 64$). The indices m and n are running from $-L/2$ to $L/2$, corresponding to the first Brillouin zone. The constant $g_2 = \sum_{\mathbf{q}\neq 0} G^2(\mathbf{q})/N^2 = 3.8667 \times 10^{-3}$. The first moment $\langle B^\alpha_{loc}\rangle$ is a free parameter in the model of Bramwell *et al*. and depends on the reduced temperature $\tau = k_B T/J$: $|\langle B^\alpha_{loc}\rangle| = \Delta/(1 + 0.5 g_2 \tau^2)$.[22] Here, J is the exchange integral between neighboring spins. For highly frustrated magnetic systems τ can reach values significantly lower than unity. Thus for $\tau < 1$, we have $|\langle B^\alpha_{loc}\rangle| \simeq \Delta$.

Figure 1 displays $\Delta \times D_c(B^\alpha_{loc})$, the real and imaginary parts of $G(t)$, and $P^{stat}_Z(t)$ computed from the characteristic function written above. The short-range correlations described by the terms with $n \geqslant 3$ and $\langle B^\alpha_{loc}\rangle$ in Eq. (15) have a strong effect on $P^{stat}_Z(t)$. For $\langle B^\alpha_{loc}\rangle = 0$ the muon polarization function slightly differs from the Kubo-Toyabe function [dashed line in Fig. 1(c)]. For $\langle B^\alpha_{loc}\rangle > 0$ the minimum in the muon polarization function $P^{stat}_Z(t)$ deepens and oscillations become more pronounced. This polarization function resembles that of an ordered magnetic system with a strong damping. The situation is different for $\langle B^\alpha_{loc}\rangle < 0$. The minimum of $P^{stat}_Z(t)$ becomes shallower than for the Kubo-Toyabe function, especially for $\langle B^\alpha_{loc}\rangle \simeq -0.5\Delta$ when the maximum of the component field distribution $\Delta \times D_c(B^\alpha_{loc})$ is close to $B^\alpha_{loc} = 0$.

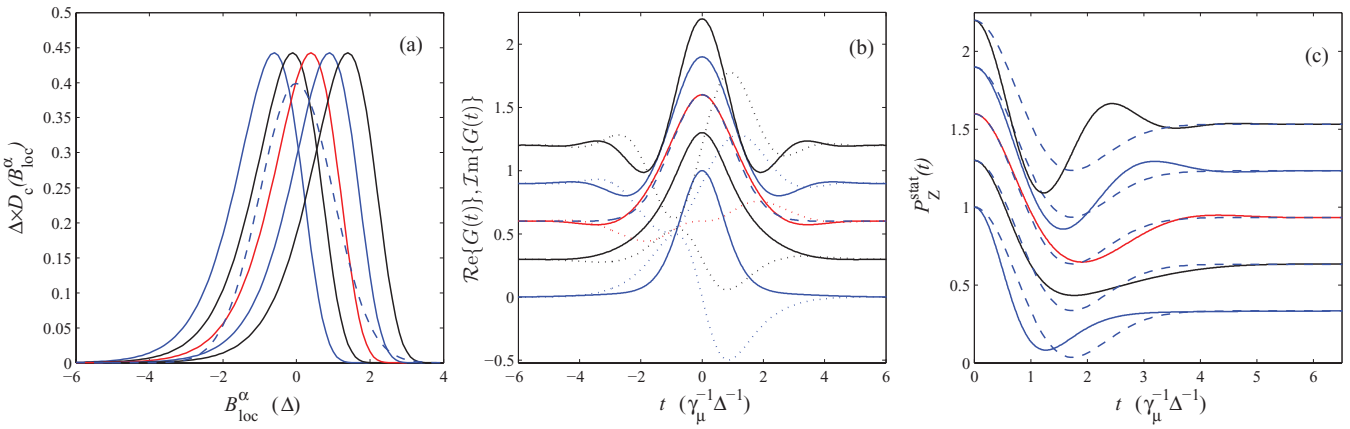

FIG. 1. (Color online) (a) The normalized component field distributions $\Delta \times D_c(B^\alpha_{loc})$ of the low-temperature phase of the two-dimensional XY model computed using Eqs. (17) and (18) for $\langle B^\alpha_{loc}\rangle = -\Delta, -0.5\Delta, 0, 0.5\Delta$, and Δ (from left to right). Note that the field is given in units of Δ. For this model the skewness and excess kurtosis are equal to -0.8907 and 4.415, respectively. The corresponding real and imaginary parts of $G(t)$, solid and dotted lines, respectively, are presented in panel (b), and $P^{stat}_Z(t)$ in panel (c). For better visualization each plot of the $G(t)$ and $P^{stat}_Z(t)$ functions is shifted by 0.3 units. The time t is in units of $1/(\gamma_\mu\Delta)$. The dashed lines refer to functions when the correlations are neglected; e.g., we plot the Kubo-Toyabe function in panel (c).

The method we have just described to compute $P_Z^{\rm stat}(t)$ requires $G(t)$ to be known, and not just few of its first moments. This is because the bounds of the integral in Eq. (7) run from minus infinity to infinity, and therefore an extremely large number of terms of the Maclaurin expansion is needed. However, $G(t)$ is rarely known theoretically. In fact, it is usually the purpose of measurements to determine it. Therefore we need a more general method to account for the short-range spin correlations. Instead of working with $G(t)$, we directly consider the component-field distribution. We write

$$D_{\rm c}\left(B_{\rm loc}^{\alpha}\right) = \frac{1}{N\delta}\exp\left[-g\left(B_{\rm loc}^{\alpha}/\delta\right)\right], \tag{19}$$

where $N\delta$ normalizes $D_{\rm c}(B_{\rm loc}^{\alpha})$ with

$$N = \int_{-\infty}^{\infty}\exp[-g(x)]dx \tag{20}$$

and

$$g(x) = \tfrac{1}{2}x^2 + \tfrac{1}{3}(\eta_3 x)^3 + \tfrac{1}{4}(\eta_4 x)^4. \tag{21}$$

We only need to consider $\eta_3 \geqslant 0$ and $\eta_4 > 0$ to cover all the physical cases. The distribution depends on three free parameters: δ in units of field and the two unitless parameters η_3 and η_4. The eventual asymmetry resulting from the spin correlations is accounted for by the third-order term gauged by the asymmetry parameter η_3. The fourth-order term alone is the minimum extension from a Gaussian distribution. It is required for the convergence of the integral in Eq. (20) if the third-order term is present. The distribution $D_{\rm c}(B_{\rm loc}^{\alpha})$ has a single or several maximums depending on the value of the η_3 and η_4 parameters. To determine the condition of occurrence of a single maximum we define the function $f(x)$ through the relation

$$\frac{dg(x)}{dx} = xf(x). \tag{22}$$

We compute

$$f(x) = \eta_4^4 x^2 + \eta_3^3 x + 1. \tag{23}$$

$g(x)$ has a single minimum at $x = 0$ provided that the discriminant of the $f(x)$ polynomial is negative; i.e.,

$$\eta_3 < 2^{1/3}\eta_4^{2/3}. \tag{24}$$

When this condition is fulfilled $D_{\rm c}(B_{\rm loc}^{\alpha})$ has a single peak.

Since $D_{\rm c}(B_{\rm loc}^{\alpha})$ is defined, $G(t)$ can be derived from Eq. (4) for different $\{\eta_3,\eta_4\}$ pairs, as well as $P_Z^{\rm stat}(t)$ in zero field from Eq. (3) or Eq. (5). It is interesting to note that numerical calculations of the $P_Z^{\rm stat}(t)$ functions with Eq. (5) yield a result which is distinct from that obtained with Eq. (3) for all $\eta_3 \neq 0$ or $\eta_4 \neq 0$. For $\eta_3 \neq 0$ this result is obvious, since Eqs. (5) and (6) do not account for the imaginary part of the characteristic function. However, the golden formula due to Kubo [Eq. (5)] is also not valid for $\eta_3 = 0$ and $\eta_4 \neq 0$, i.e., when the imaginary part vanishes (see Fig. 2). Therefore, for the calculations discussed below we use the standard definition of the $P_Z^{\rm stat}(t)$ function expressed with Eq. (3). Results are presented in Figs. 2, 3, and 4.

In Fig. 2 $\delta \times D_{\rm c}(B_{\rm loc}^{\alpha})$, $G(t)$, and $P_Z^{\rm stat}(t)$ are displayed for different η_4 values with $\eta_3 = 0$. Obviously the deviation of $\delta \times D_{\rm c}(B_{\rm loc}^{\alpha})$ and $G(t)$ from Gaussian behaviors increases with η_4. The $P_Z^{\rm stat}(t)$ minimum also deepens, and correlatively the function presents a structure which could be taken as an indication of an oscillation just before the 1/3 plateau is reached. This could be mistaken as a signature of a finite mean field, although the mean field is zero by construction. To determine whether such a field does exist the measurement of its temperature dependence could be useful. In addition, an estimate of the correlation length of the involved magnetic structure could help to decide whether or not there is effectively a finite mean field.[16]

In Figs. 3 and 4 we show the dependence of the functions $\delta \times D_{\rm c}(B_{\rm loc}^{\alpha})$, $G(t)$, and $P_Z^{\rm stat}(t)$ on η_3 for three η_4 values. Systematically, we plot the functions as deduced either directly from Eq. (19), or setting the mean field to zero; i.e., $g[B_{\rm loc}^{\alpha}/\delta]$ is replaced with $g[(B_{\rm loc}^{\alpha} - \langle B_{\rm loc}^{\alpha}\rangle)/\delta]$ in Eq. (19). Physical cases with vanishing mean field even in the ordered state of magnets have been found for geometrically frustrated

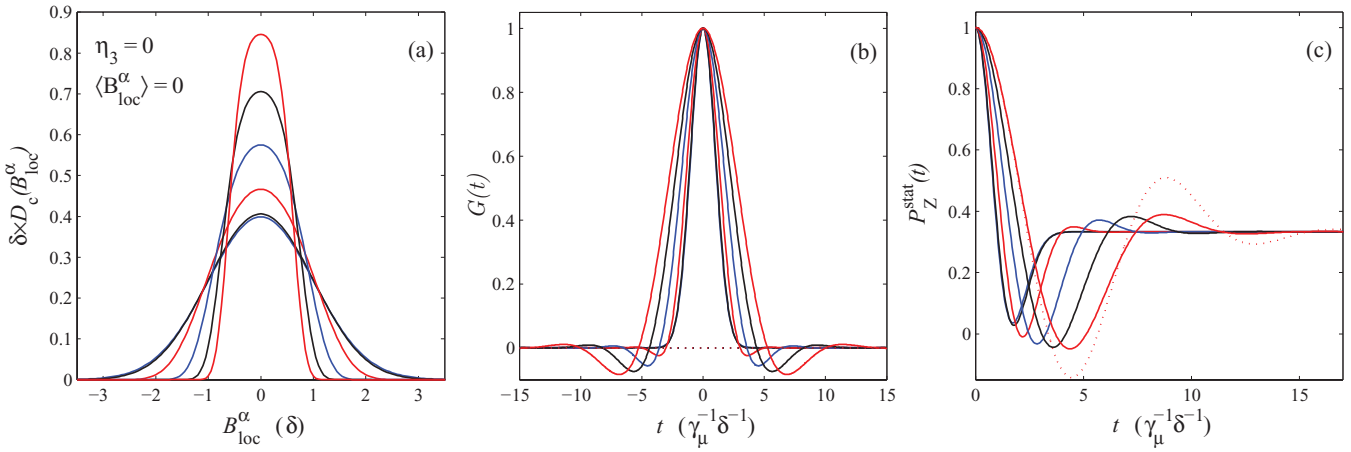

FIG. 2. (Color online) Dependence of the normalized component field distribution $\delta \times D_{\rm c}(B_{\rm loc}^{\alpha})$ given by Eq. (19) (a), the related characteristic function $G(t)$ which is real (b), and zero-field polarization function $P_Z^{\rm stat}(t)$ (c) on η_4 with η_3 set to zero. The curves are for $\eta_4 = 0$, 0.4, 0.8, 1.2, 1.6, and 2.0. The field is in units of δ and the time in $1/(\gamma_\mu\delta)$. The dotted line in panel (c) shows the $P_Z^{\rm stat}(t)$ function calculated with Eq. (5) for $\eta_3 = 0$ and $\eta_4 = 2.0$. The strong deviation from the corresponding result obtained with Eq. (3) is obvious.

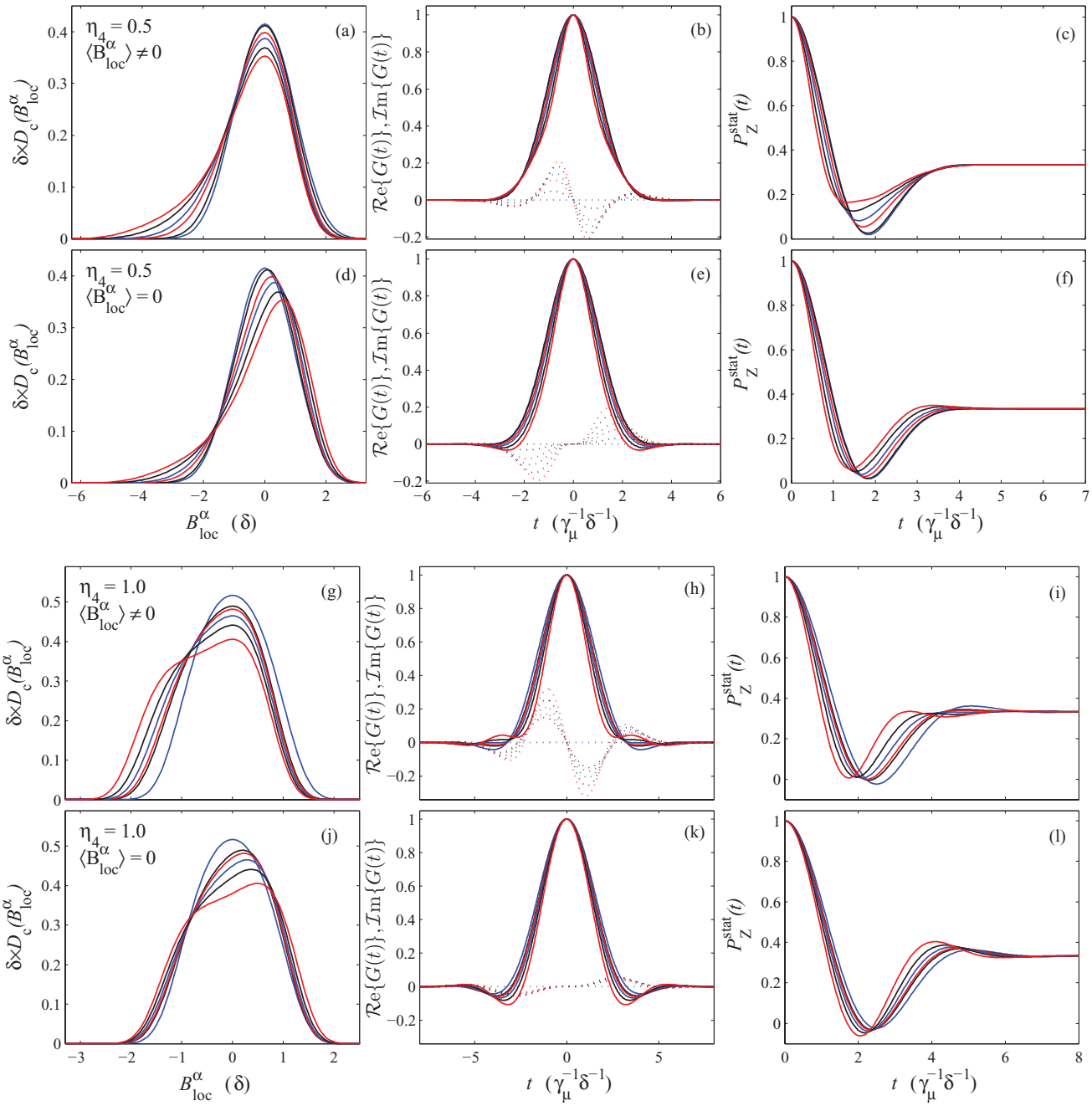

FIG. 3. (Color online) Dependence of the component field distribution $\delta \times D_c(B^\alpha_{loc})$ [panels (a), (d), (g), and (j)], the real and imaginary parts of the characteristic function $G(t)$, solid and dotted lines, respectively [panels (b), (e), (h), and (k)], and the related zero-field polarization function $P_Z^{stat}(t)$ [panels (c), (f), (i), and (l)] on η_4 and η_3. The drawings in the upper two panels are for $\eta_4 = 0.50$ with $\eta_3 = 0, 0.50, 0.65, 0.70, 0.74$, and 0.76. In the lower two panels we present data for $\eta_4 = 1.0$ with $\eta_3 = 0, 1.00, 1.04, 1.10, 1.16$, and 1.22. For each $\{\eta_3, \eta_4\}$ pair, the mean field $\langle B^\alpha_{loc}\rangle$ is set to zero in the lower panels. The units are as in Fig. 2.

magnetic materials.[23–25] A minimum for $P_Z^{stat}(t)$ is always present at relatively short time. Depending on the parameters it is more or less deep and wide. Again a structure which could be mistaken as an indication of an oscillation may precede the 1/3 plateau. It may be taken as a signature of a finite mean field even if it does not exist. Therefore caution should be exercised in interpreting μSR data. As explained in Ref. 16, from the analysis of the oscillation it is possible to estimate its associated correlation length, and therefore to determine whether it is reasonable to attribute the structure to a long-range magnetic ordering.

We have described $P_Z^{stat}(t)$ in zero field, i.e., when $\mathbf{B}_{ext} = \mathbf{0}$. As explained in Ref. 16, to account for $\mathbf{B}_{ext}$ we simply need to substitute Eq. (2) with

$$D_{v,\mathbf{B}_{ext}}(\mathbf{B}_{loc}) d^3\mathbf{B}_{loc} = D_c\left(B^X_{loc}\right) D_c\left(B^Y_{loc}\right) D_c\left(B^Z_{loc} - B_{ext}\right) \times dB^X_{loc} dB^Y_{loc} dB^Z_{loc}, \quad (25)$$

and replace $D_v(\mathbf{B}_{loc})$ with $D_{v,\mathbf{B}_{ext}}(\mathbf{B}_{loc})$ in Eq. (1).

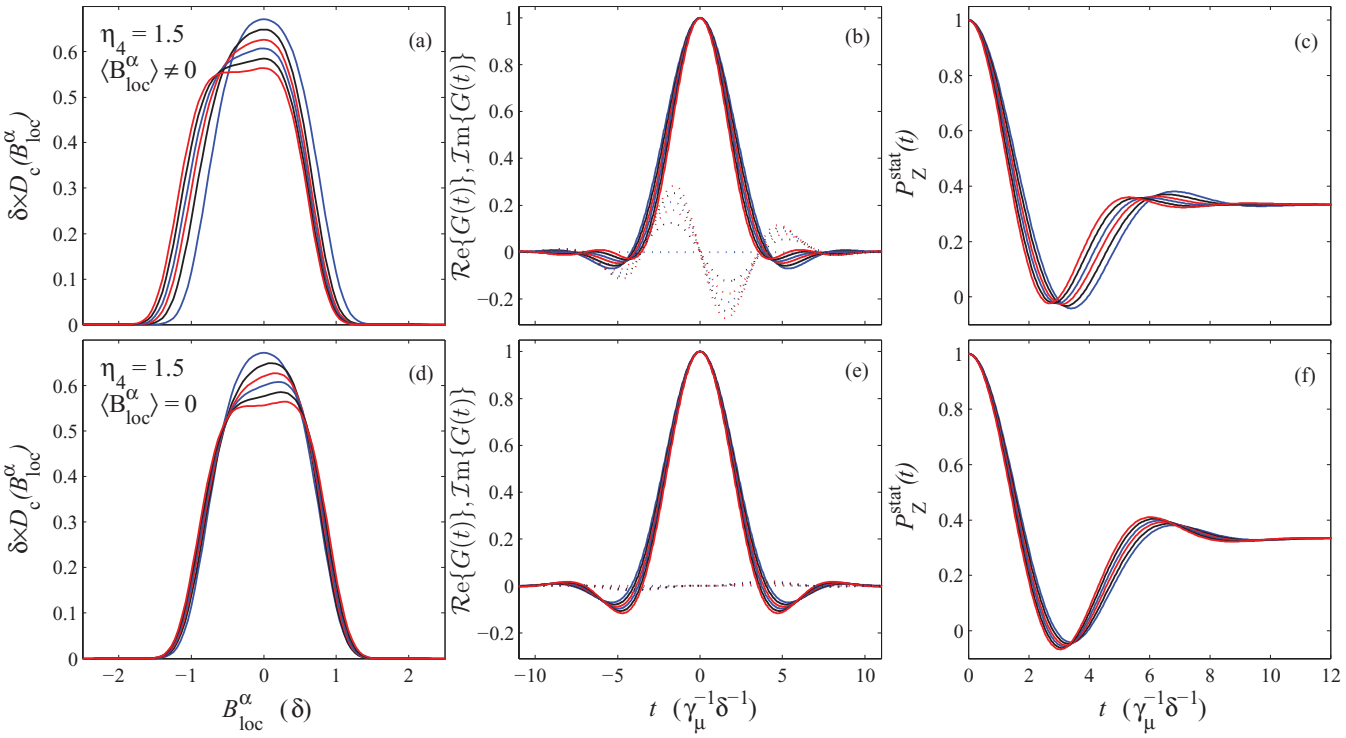

FIG. 4. (Color online) Same caption as in Fig. 3, but for $\eta_4 = 1.50$ with $\eta_3 = 0, 1.30, 1.45, 1.53, 1.60$, and 1.65.

Up to now we have only discussed $P_\alpha^{\rm stat}(t)$. To account for the spin dynamics, and therefore to compute $P_\alpha(t)$, the simplest method is to use the so-called strong collision model for which $P_\alpha(t)$ is expressed in terms of an integral equation:[16,26,27]

$$P_\alpha(t) = P_\alpha^{\rm stat}(t)\exp(-\nu_{\rm c}t) + \nu_{\rm c}\int_0^t P_\alpha(t-t')P_\alpha^{\rm stat}(t') \times \exp(-\nu_{\rm c}t')dt', \quad (26)$$

where $\nu_{\rm c} = 1/\tau_{\rm c}$ is the magnetic correlation frequency and $\tau_{\rm c}$ the magnetic correlation time. The strong collision model is a reasonable approximation for three-dimensional magnetic systems, and it is known to break down for one-dimensional magnetic systems.

Experimentally, $P_Z(t)$ and $P_X(t)$ are measured. Their analysis with Eq. (19) gives access to the component-field distribution described in general by four parameters: $\nu_{\rm c}$ and the three parameters for the static field distribution, i.e., δ, ν_3, and ν_4. Using Eqs. (11) and (13), the mean field, standard deviation, skewness, and kurtosis, and therefore excess kurtosis, can be estimated, and the corresponding characteristic function can be computed with Eq. (4) using the experimentally determined component field distribution.

As an example we shall analyze the longitudinal μSR asymmetry signal measured in the quantum-spin-liquid phase of the pyrochlore $Yb_2Ti_2O_7$.[3] Controversial experimental results have been obtained for this pyrochlore oxide. Depending on the single-crystal sample, magnetic Bragg reflections at low temperature are present[28,29] or absent.[30–33] Recent studies show the variability of the response of the system.[34,35] No magnetic reflections are detected for a powder sample with a well-developed specific-heat anomaly,[3] much more intense than in the best available single crystal.[28] In fact, a $Yb_2Ti_2O_7$ powder sample only displays short-range magnetic correlations. This is a characteristic of the compound since according to neutron diffraction[35] only a powder sample is stoichiometric.

Because a Yb^{3+} ion in this compound is characterized by a well-isolated Kramers doublet ground state, and since the Ising exchange interaction is strong and positive, $Yb_2Ti_2O_7$ could be a quantum spin-liquid system discussed in the framework of the quantum spin-ice model.[36] In Fig. 5 we present the measured asymmetry for the powder sample, i.e., $a_0 P_Z^{\rm exp}(t)$.[3] It is described by the weighted sum $a_0 P_Z^{\rm exp}(t) = a_{\rm s} P_Z(t) + a_{\rm bg}$, where the constant $a_{\rm bg} = 0.069(1)$ accounts for the muon stopping in the silver sample holder and in the cryostat. A weak longitudinal field $B_{\rm ext} = 2$ mT was applied to quench the possible effect of the nuclear magnetic moments of the ^{47}Ti, ^{49}Ti, ^{171}Yb, and ^{173}Yb isotopes. For the analysis of the experimental time spectrum the component field distribution was evaluated using Eqs. (19)–(21); next, the static muon polarization function was calculated with Eqs. (25) and (3) (i.e., considering the small external longitudinal field $B_{\rm ext}$); and finally, the spin dynamics was accounted for with Eq. (26). The result is shown in Fig. 5. Usage of identical component field distributions for the three directions, i.e., $\alpha = \{X, Y, Z\}$, is justified since $Yb_2Ti_2O_7$ has a cubic crystal structure and the μSR asymmetry was measured on a powder sample. The fit yields the following values of parameters: $\delta = 3.24(15)$ mT, $\eta_3 = 0.784(3)$, $\eta_4 = 0.50(1)$, $\nu_{\rm c} = 0.97(6)$ μs^{-1}, and $a_{\rm s} = 0.161(4)$. We have checked numerically that the small $B_{\rm ext}$ value has a negligible effect on these parameters, since the local fields probed by the muons are significantly larger (see Fig. 5).

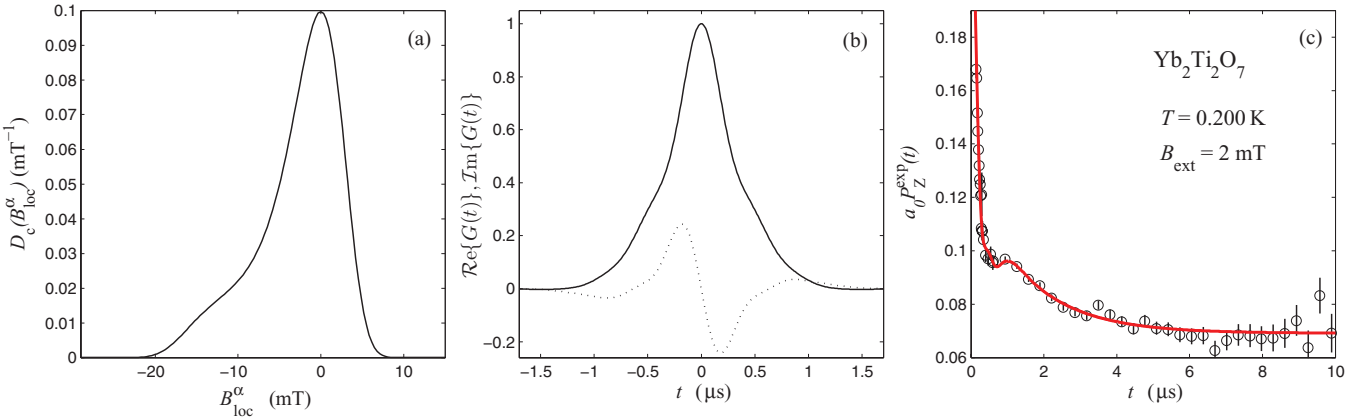

FIG. 5. (Color online) Analysis of the μSR time spectrum measured at 0.200 K and in a 2 mT longitudinal field for a powder sample of $Yb_2Ti_2O_7$ (Ref. 3) $a_0 P_Z^{exp}(t)$ is shown in panel (c) (circles). The solid line is the best fit of the data using Eqs. (19), (25), (3), and (26) (see main text). The real (solid line) and imaginary (dotted line) parts of $G(t)$ are shown in panel (b). Corresponding $D_c(B^\alpha_{loc})$ function is depicted in panel (a).

The inequality given in Eq. (24) is effectively obeyed since $2^{1/3}\eta_4^{2/3} = 0.798 > 0.784(3) = \eta_3$; then the distribution has a single maximum. The description of the measured spectrum is excellent. As expected, $D_c(B^\alpha_{loc})$ is found extremely asymmetric; see left panel of Fig. 5. In the middle panel of the figure are plotted the real and imaginary parts of $G(t)$. Originally the spectrum was analyzed in terms of three parameters using the phenomenological model of Noakes and Kalvius:[2] a standard deviation, a ratio of standard deviations, and ν_c. This model is not justified physically. In contrast the present model is based on fundamental statistical principles and introduces four parameters: a standard deviation, a skewness, a kurtosis, and ν_c. We have computed the first four moments of the measured component field distribution, and deduced from them the mean field, standard deviation, skewness, and excess kurtosis. We find $\langle B^\alpha_{loc}\rangle = -2.82(3)$ mT, $\Delta = 5.07(10)$ mT, $\nu_3 = -0.89(4)$, and $\tilde{\nu}_4 = 3.35(17)$. Interestingly, $\langle B^\alpha_{loc}\rangle$ is nonzero. This reflects the field asymmetry with its pronounced tail in the negative field region. It is only the present analysis which enables us to unravel information on the field distribution, such as its asymmetry and the finite $\langle B^\alpha_{loc}\rangle$ value. That could not be done with the previous phenomenological analysis of the spectrum.[3] A Hamiltonian has been proposed for the description of $Yb_2Ti_2O_7$.[37,38] It would be interesting to compute its $G(t)$ function, or at least its first moment, standard deviation, skewness, and excess kurtosis. To compare the computational and experimental results, the dipole coupling between the muon moment and the Yb^{3+} moments has to be described. As examples of computation of moments of Hamiltonian operators, we refer to Bramwell *et al.* who used classical mechanics,[19] and the well-known work of Van Vleck for the second moment of a nuclear magnetic resonance line.[39]

In conclusion, in this report we have proposed two methods to account for the short-range spin correlations for the two basic μSR polarization functions in the slow dynamic limit. In the lucky case for which the characteristic function of the Hamiltonian of the system under study is known, we explain how to compute the polarization functions. In most cases of interest the available information on the system is quite restricted, and the μSR measurements are expected to yield useful information. We explain how the polarization functions can be analyzed to deduce the characteristic function and to extract parameters such as the standard deviation, skewness, and excess kurtosis of the Hamiltonian. To round up our discussion, we analyze the published low-temperature longitudinal field spectrum measured in the quantum-spin-liquid phase of $Yb_2Ti_2O_7$. This enables us to get information on the field distribution at the muon site, and therefore to determine the characteristic function and values of the first four moments.

This work was partly supported by NCCR MaNEP sponsored by the Swiss National Science Foundation.

[1] Y. J. Uemura, T. Yamazaki, D. R. Harshman, M. Senba, and E. J. Ansaldo, Phys. Rev. B **31**, 546 (1985).
[2] D. R. Noakes and G. M. Kalvius, Phys. Rev. B **56**, 2352 (1997).
[3] J. A. Hodges, P. Bonville, A. Forget, A. Yaouanc, P. Dalmas de Réotier, G. André, M. Rams, K. Królas, C. Ritter, P. C. M. Gubbens *et al.*, Phys. Rev. Lett. **88**, 077204 (2002).
[4] G. Ehlers, J. Phys.: Condens. Matter **18**, R231 (2006).
[5] J. Lago, S. J. Blundell, and C. Baines, J. Phys.: Condens. Matter **19**, 326210 (2007).
[6] J. S. Gardner, G. Ehlers, P. Fouquet, B. Farago, and J. R. Stewart, J. Phys.: Condens. Matter **23**, 164220 (2011).
[7] J. A. Hodges, P. Dalmas de Réotier, A. Yaouanc, P. C. M. Gubbens, P. J. C. King, and C. Baines, J. Phys.: Condens. Matter **23**, 164217 (2011).
[8] D. R. Noakes, J. Phys.: Condens. Matter **11**, 1589 (1999).
[9] A. Schenck and F. N. Gygax, in *Handbook of Magnetic Materials*, edited by K. H. J. Buschow (Elsevier, Amsterdam, 1995), Vol. 9.

[10]P. Dalmas de Réotier and A. Yaouanc, J. Phys.: Condens. Matter **9**, 9113 (1997).
[11]G. M. Kalvius, D. R. Noakes, and O. Hartmann, in *Handbook on the Physics and Chemistry of Rare Earths*, edited by K. A. Gschneidner, L. Eyring, and G. H. Lander (North-Holland, Amsterdam, 2001), Vol. 32.
[12]M. Pinkpank, A. Amato, D. Andreica, F. N. Gygax, H. R. Ott, and A. Schenck, Physica B **289–290**, 295 (2000).
[13]A. Abragam, *The Principles of Nuclear Magnetism* (Clarendon, Oxford, 1960).
[14]C. P. Slichter, *Principles of Magnetic Resonance* (Springer, Berlin, 1996), third enlarged and updated edition.
[15]P. Dalmas de Réotier, P. C. M. Gubbens, and A. Yaouanc, J. Phys.: Condens. Matter **16**, S4687 (2004).
[16]A. Yaouanc and P. Dalmas de Réotier, *Muon Spin Rotation, Relaxation, and Resonance: Applications to Condensed Matter*, International Series of Monographs on Physics 147 (Oxford University Press, Oxford, 2011).
[17]H. Cramér, *Mathematical Methods of Statistics* (Princeton University Press, Princeton, 1999), nineteenth printing.
[18]N. G. van Kampen, *Stochastic Processes in Physics and Chemistry* (North-Holland, Amsterdam, 1981).
[19]S. T. Bramwell, T. Fennell, P. C. W. Holdsworth, and B. Portelli, Europhys. Lett. **57**, 310 (2002).
[20]R. Kubo, Hyperfine Interact. **8**, 731 (1981).
[21]T. Yamazaki, Hyperfine Interact. **104**, 3 (1997).
[22]S. T. Bramwell, J.-Y. Fortin, P. C. W. Holdsworth, S. Peysson, J.-F. Pinton, B. Portelli, and M. Sellitto, Phys. Rev. E **63**, 041106 (2001).
[23]P. Dalmas de Réotier, A. Yaouanc, L. Keller, A. Cervellino, B. Roessli, C. Baines, A. Forget, C. Vaju, P. C. M. Gubbens, A. Amato *et al*., Phys. Rev. Lett. **96**, 127202 (2006).
[24]J. Lago, T. Lancaster, S. J. Blundell, S. T. Bramwell, F. L. Pratt, M. Shirai, and C. Baines, J. Phys.: Condens. Matter **17**, 979 (2005).
[25]P. Dalmas de Réotier, A. Yaouanc, D. E. MacLaughlin, S. Zhao, T. Higo, S. Nakatsuji, Y. Nambu, C. Marin, G. Lapertot, A. Amato *et al*., Phys. Rev. B **85**, 140407 (2012).
[26]K. W. Kehr, G. Honig, and D. Richter, Z. Phys. B **32**, 49 (1978).
[27]R. S. Hayano, Y. J. Uemura, J. Imazato, N. Nishida, T. Yamazaki, and R. Kubo, Phys. Rev. B **20**, 850 (1979).
[28]L.-J. Chang, S. Onoda, Y. Su, Y.-J. Kao, K.-D. Tsuei, Y. Yasui, K. Kakurai, and M. R. Lees, Nat. Commun. **3**, 992 (2012).
[29]Y. Yasui, M. Soda, S. Iikubo, M. Ito, M. Sato, N. Hamaguchi, T. Matsushita, N. Wada, T. Takeuchi, N. Aso *et al*., J. Phys. Soc. Jpn. **72**, 3014 (2003).
[30]P. Bonville, J. A. Hodges, E. Bertin, J.-P. Bouchaud, P. Dalmas de Réotier, L.-P. Regnault, H. M. Rønnow, J.-P. Sanchez, S. Sosin, and A. Yaouanc, Hyperfine Interact. **156–157**, 103 (2004).
[31]J. S. Gardner, G. Ehlers, N. Rosov, R. W. Erwin, and C. Petrovic, Phys. Rev. B **70**, 180404(R) (2004).
[32]K. A. Ross, J. P. C. Ruff, C. P. Adams, J. S. Gardner, H. A. Dabkowska, Y. Qiu, J. R. D. Copley, and B. D. Gaulin, Phys. Rev. Lett. **103**, 227202 (2009).
[33]K. A. Ross, L. R. Yaraskavitch, M. Laver, J. S. Gardner, J. A. Quilliam, S. Meng, J. B. Kycia, D. K. Singh, T. Proffen, H. A. Dabkowska *et al*., Phys. Rev. B **84**, 174442 (2011).
[34]A. Yaouanc, P. Dalmas de Réotier, Y. Chapuis, C. Marin, S. Vanishri, D. Aoki, B. Fåk, L. P. Regnault, C. Buisson, A. Amato *et al*., Phys. Rev. B **84**, 184403 (2011).
[35]K. A. Ross, T. Proffen, H. A. Dabkowska, J. A. Quilliam, L. R. Yaraskavitch, J. B. Kycia, and B. D. Gaulin, Phys. Rev. B **86**, 174424 (2012).
[36]L. Savary and L. Balents, Phys. Rev. Lett. **108**, 037202 (2012).
[37]K. A. Ross, L. Savary, B. D. Gaulin, and L. Balents, Phys. Rev. X **1**, 021002 (2011).
[38]R. Applegate, N. R. Hayre, R. R. P. Singh, T. Lin, A. G. R. Day, and M. J. P. Gingras, Phys. Rev. Lett. **109**, 097205 (2012).
[39]J. H. Van Vleck, Phys. Rev. **74**, 1168 (1948).